Acta Mech Sinica (2005) 21, 103–111
DOI 10.1007/s10409-005-0019-9

RESEARCH PAPER

Markus J. Buehler · Alexander Hartmaier
Mark A. Duchaineau · Farid F. Abraham · Huajian Gao

The dynamical complexity of work-hardening: a large-scale molecular dynamics simulation

Received: 3 November 2004 / Accepted: 24 November 2004 / Published online: 7 April 2005

Abstract We analyze a large-scale molecular dynamics simulation of work hardening in a model system of a ductile solid. With tensile loading, we observe emission of thousands of dislocations from two sharp cracks. The dislocations interact in a complex way, revealing three fundamental mechanisms of work-hardening in this ductile material. These are (1) dislocation cutting processes, jog formation and generation of trails of point defects; (2) activation of secondary slip systems by Frank-Read and cross-slip mechanisms; and (3) formation of sessile dislocations such as Lomer-Cottrell locks. We report the discovery of a new class of point defects referred to as trail of partial point defects, which could play an important role in situations when partial dislocations dominate plasticity. Another important result of the present work is the rediscovery of the Fleischer-mechanism of cross-slip of partial dislocations that was theoretically proposed more than 50 years ago, and is now, for the first time, confirmed by atomistic simulation. On the typical time scale of molecular dynamics simulations, the dislocations self-organize into a complex sessile defect topology. Our analysis illustrates numerous mechanisms formerly only conjectured in textbooks and observed indirectly in experiments. It is the first time that such a rich set of fundamental phenomena have been revealed in a single computer simulation, and its dynamical evolution has been studied. The present study exemplifies the simulation and analysis of the complex nonlinear dynamics of a many-particle system during failure using ultra-large scale computing.

Keywords Work-hardening · Large-scale atomistic simulation · Dislocation junction · Cross-slip

M. J. Buehler
California Institute of Technology, 1201 East California Blvd., Pasadena, 91125, CA, USA

M.J. Buehler · A. Hartmaier · H. Gao (✉)
Max Planck Institute for Metals Research, Heisenbergstrasse 3, D-70569 Stuttgart, Germany
E-mail: hjgao@mf.mpg.de
Fax: ++49 711 689 3512

M.A. Duchaineau
Lawrence Livermore National Laboratory, 7000 East Ave., Livermore, CA, 94550, USA

F.F. Abraham
IBM Almaden Research Center, 650 Harry Road, San Jose, CA, 95120, USA

1 Introduction

The plastic or non-reversible deformation of materials occurs immediately after a regime of recoverable elastic deformations and is governed by the nucleation and motion of defects in the crystal lattice [1–3]. In experiment, researchers often rely on indirect techniques to investigate the creation and interaction of defects. In theory, predictions are primarily based on continuum theory with phenomenological assumptions. While the continuum description has been very successful in the past, some of the key features of plasticity can only be understood when the atomistic viewpoint is taken into account, and this may be achieved using atomistic simulation methods, like molecular dynamics (MD) [4–14]. However, most MD studies consider a small number of dislocations and address specific dislocation mechanisms, such as cross slip or dislocation cutting processes [15–19], dislocation nucleation from cracks and dislocation reactions [20, 21]. Large-scale studies of plastic deformation incorporating several hundred million atoms where all dislocation mechanisms appear concurrently have not been achieved up to date.

With the advent of teraflop computers, scientists are able to simulate billions of atoms on the nanosecond scale [5]. System sizes on the order of micrometer are critical such that insight into the concurrent dynamics of different dislocation mechanics can be gained.

We present an analysis of a 500 million-atom simulation of work hardening in a model system for ductile copper. The main objective of this simulation is to provide a detailed analysis of the concurrent dynamics of dislocation and defect interaction mechanisms during the failure. The simulation geometry, lattice orientation and coordinate system are presented in Figs. 1(a) and 1(b). By applying tensile loading, two

sharp cracks serve as fertile sources for thousands of dislocations. This simulation setup is identical to that previously used by some of the authors of the present paper. In contrast to the earlier publication that included only a superficial analysis of the failure process [5], in the present work we achieve, for the first time, a detailed atomic scale analysis of the complex dynamical evolution of the defect structure (including quantitative determination of Burgers vectors, line direction etc.). This helps to understand several important questions of the defect evolution, such as, for instance, the Burgers vectors of the involved dislocations, the cross-slip mechanism, the details of sessile lock formation, the dislocation cutting processes, as well as a description of the particular structure of the final defect network [5]. The analysis reveals that the dislocation interactions develop a rigid network of sessile defects with a complex topology. We find that there exist three mechanisms of interactions between dislocations. These are (1) dislocation cutting processes with point defect generation, (2) activation of secondary slip systems by cross-slip and Frank-Read mechanisms, and (3) formation of sessile Lomer-Cottrell locks. Eventually, a final rigid structure consisting of point defects, sessile dislocation locks and glissile partial dislocations develops. We analyze and describe this final structure, and show full atomistic details of the fundamental mechanisms of hardening. We further present a statistical analysis of the densities of the different defects and their dynamical evolution, and correlate these with the observed interaction mechanisms.

Although many of the mechanisms we find have been described by MD simulations in previous publications (see, for instance [22–24]), this is the first time that such a rich set of fundamental phenomena are being seen within a single computer simulation, thus allowing insight into the dynamical evolution of the different mechanisms. Also, the level of detail of the present analysis has, to the best of our knowledge, not been achieved in any prior published work.

The analysis validates and underlines the power of continuum mechanics theories [1,2] in predicting the properties and interactions of topological defects in lattices, as the observed effects can all be explained by the classical theories. Figure 1(c) shows a time sequence of an overview of the work-hardening simulation.

2 Atomistic model

2.1 Computer experiment setup

Our model for simulating work-hardening is very simple. We consider two opposing surface cracks on opposite faces of a three-dimensional FCC solid cube (Figs. 1(a) and (b)). The system is a slab with 1 008 atoms along the x and y orthogonal sides and 504 atoms along the z direction. Two notches are centred midway along the x-direction, along the cube faces at $y = 0$ and $y = L_y$, with a y-extension of 90 atomic layers extending though the entire thickness L_z. The exposed notch faces are in the y-z planes with (110) faces, and the notch is pointed in the $\langle 1\bar{1}0 \rangle$ direction. Periodic boundary conditions are imposed between the x-y faces at $z = 0$ and $z = L_z$. This notched slab geometry has a total of 511 551 936 atoms.

2.2 Simulation tool and boundary conditions

Our simulation tool is classical molecular dynamics, one of the simplest, yet most powerful atomistic simulation tools in computational physics. Molecular dynamics allows the prediction of the motion of a large number of atoms governed by their mutual interatomic interaction, and it requires the numerical integration of the Newtonian equations of motion [4] $F = ma$.

In the present simulations, we adopt a simple interatomic force law since we wish to investigate the generic features of a particular many-body problem common to a large class of real physical systems and not governed by the particular complexities of a unique molecular interaction. The model potential for the present study is the Lennard-Jones (LJ) potential [4]. With its well-known shortcomings, it nevertheless provides a fundamental description of the generic features of interatomic interaction: Atomic repulsion at close distances, and attraction at large radii of separation. A similar approach of using model potentials to study the essential physics of fracture was recently taken successfully in a study of deformation of brittle materials, where a new length scale in dynamic fracture was discovered [7].

The slab (Figs. 1(a) and (b)) is initialized to zero temperature, and an outward strain of 4% is imposed on the outer most columns of atoms defining the opposing vertical y-z-faces of the slab, and kept constant throughout the simulation. The initial purely elastic strain is relaxed into plastic strain during the course of the simulation. Since we use an NVE ensemble, the relief of the potential energy causes an increase of temperature in the crystal.

This simulation is very similar to the work-hardening simulation reported earlier [5], but in this study, positions and velocities of all of the atoms are stored for a central spatial region equal to approximately one tenth of the total computational cell. This is necessary so that a critical analysis of the defects' evolution can be performed. The total simulation time for this study is 200 000 MD time-steps.

2.3 Visualisation procedure and analysis techniques

In order to see into the interior of the solid, we show only those atoms that have potential energy greater than or equal to -6.1, where the ideal bulk value is -6.3. This trick was used very effectively in our earlier studies using a single crack for displaying dislocations, microcracks and other imperfections in crystal packing [5]. This reduces the number of atoms seen by approximately two orders of magnitude in 3D; the visible atoms are associated with faces of the slab and initial notch, surfaces created by crack motion, local interplanar separation associated with the material's dynamic failure at the tip, and topological defects created in the otherwise perfect crystal.

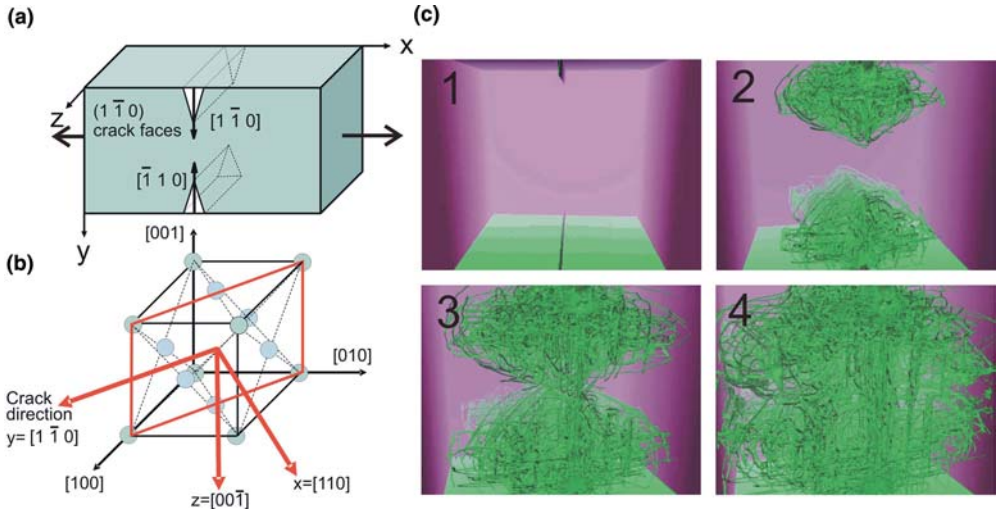

Fig. 1 Simulation geometry, lattice orientation and time-sequence of the work-hardening simulation. (**a**) Simulation geometry and (**b**) lattice orientation, also defining the directions for the x, y, z coordinate system. (**c**) Time sequence of the work-hardening simulation based on an energy analysis. Partial dislocations and other crystal defects appear as green lines. The snapshots present an overview over the total simulation and show how a large number of dislocations are created at the crack tips, flowing into the material, eventually leading to build-up of a complex, entangled dislocation network

Because of periodic boundary conditions, the vertical faces are not exterior surfaces and therefore transparent.

In contrast to previous work [5] where only the energy method was used for analysis, our desire of studying the quantitative details of the failure requires to use additional analysis approaches. In the present study we thus also employ the centrosymmetry technique [26]. This technique is particularly powerful in distinguishing stacking fault regions and partial dislocations as well as point defects.

For the analysis of the failure simulation, we find that a geometrical method is another very important tool in finding fundamental information about dislocations and defects. The geometrical method is based on performing a Burgers circuit around the dislocation in order to determine its Burgers vector and line direction. For that purpose, we rotate the atomic lattice such that we are looking onto a {111}-plane, with the horizontal x axis oriented into a $\langle 110 \rangle$ direction, and the vertical y axis aligned with a $\langle 111 \rangle$ direction. To help visualize dislocations, we stretch the atomic lattice by a factor of five to ten in the $\langle 110 \rangle$ direction. We systematically rotate the atomic lattice to investigate all possible Burgers vectors. It is important to select a subvolume of the crystal that contains only one dislocation since it significantly simplifies the analysis. Similar to the textbook approach, we determine the Burgers vector by rotating the part of the crystal (containing a single dislocation) and viewing it along the possible slip directions lying in specific glide planes. We assume that slip occurs only on $\langle 111 \rangle$ planes in {110} directions, as usually found in fcc crystals (we note we have found no indication that other slip systems are activated) [1,2]. The slip plane of the dislocation can be determined either by considering the motion of the dislocation, or if the dislocation is curved, two vectors spanning the plane can be found by two linearly independent tangential vectors to the dislocation line (the slip plane is uniquely defined by the plane which contains both the line and the Burgers vector). Similar lattice rotation operations are also used to investigate the structure of point defects. This analysis is much like analysis of TEM images from "real" laboratory experiments.

All results described in the present paper are obtained by a combination of energy method, centrosymmetry method and geometrical analysis.

3 Simulation results

3.1 Loading of the system and initial creation of dislocations from the crack tips

Upon application of loading to the system, the cracks serve as fertile sources for dislocations. Within a few picoseconds, thousands of dislocations appear and flow into the interior of the solid. The dislocations from the cracks glide on two primary glide planes (111) and (11$\bar{1}$). This is in agreement with the fact that dislocations are nucleated in the direction of the largest shear stress and thus the largest Schmid factor in the K-field of the crack [1,2]. In this early stage, the dislocations glide through the initially perfect crystal without sensing any obstacles. Dislocations with the same Burgers vector and line orientation repel each other and therefore push those previously created rapidly through the crystal [1,2].

We only observe the nucleation of partial dislocations because of the very small stacking fault energy in our model material [5]. The Burgers vectors of the emitted partials are predominantly [$\bar{2}$11] and [1$\bar{2}$1] on the (111) glide plane, as well as [$\bar{2}$1$\bar{1}$] and [1$\bar{2}\bar{1}$] on the (11$\bar{1}$) glide plane. We also find some dislocations with the other two possible Burgers vectors. Assuming a positive line direction of the dislocation in the negative z direction, the Burgers vectors all have a component in the negative x direction (which is [$\bar{1}\bar{1}$0]) in the

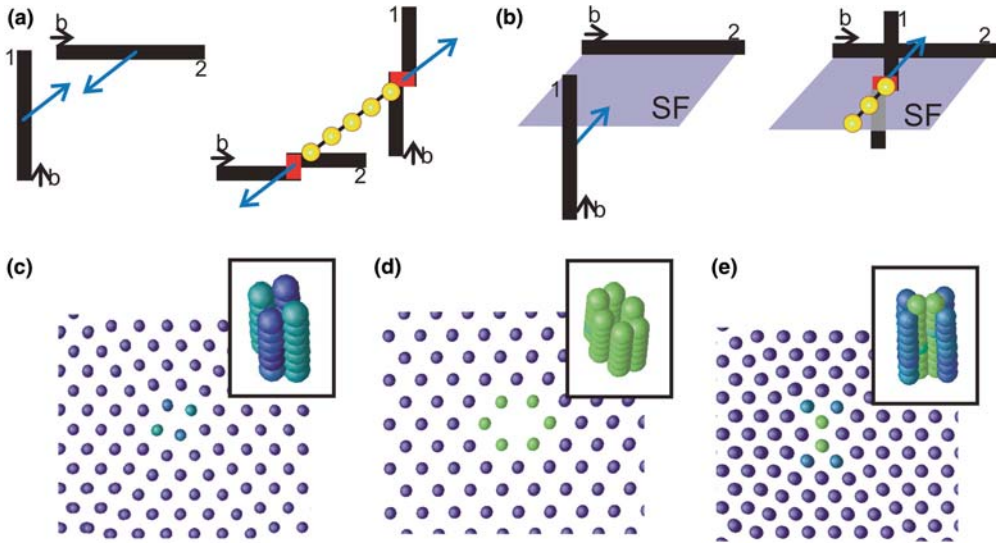

Fig. 2 Schematic of different dislocation cutting processes. Subplot (**a**) shows two partials cutting each other. Both dislocations leave a trail of point defects after intersection (yellow circles). The blue arrows indicate the velocity vectors of the dislocations. Subplot (**b**) shows a partial dislocation (black line) cutting the stacking fault (bluish region) of another partial dislocation. Dislocation number 1 leaves a trail of point defects (yellow circles) once it hits the stacking fault generated by dislocation number 2. Panels (c)–(e) show atomistic simulation results of different types of point defects: (**c**) Trail of partial point defects, (**d**) vacancy tube, and (**e**) trail of interstitials

upper cloud. In the lower cloud, the Burgers vectors have the opposite sign.

We also see dislocations on the $(\bar{1}11)$ and $(1\bar{1}1)$ glide planes in regions very close to the crack tip. However, these dislocations sense no strong elastic driving force that would allow them to flow further away from the crack tip. The dislocations on the primary glide systems (111) and $(11\bar{1})$ outrun dislocations on the $(\bar{1}11)$ and $(1\bar{1}1)$ glide planes, and in the centre of the simulation sample, only dislocations on primary glide systems occur.

3.2 Dislocation cutting processes

It is known, from the literature [1,2], that, when two screw dislocations intersect, each acquires a jog with a direction and length equal to the Burgers vector of the other dislocation. Upon intersection, the dislocations cannot glide conservatively since each jog has a sessile edge segment. However, if the applied stress is sufficiently large, the dislocations will glide, and the moving jogs will leave a trail of vacancies, or a trail of interstitials depending on the line orientation and the Burgers vector of the reacting dislocations. Generation of interstitials is energetically expensive and thus not observed frequently. The mechanism of dislocation cutting is shown in Fig. 2(a). Another possible mechanism of dislocation cutting is when a partial dislocation moves through the stacking fault generated by another partial dislocation as shown in Fig. 2(b).

Intersection of a partial dislocation with the stacking fault of another dislocation is observed in early stages when dislocations within the same cloud intersect the stacking fault generated by other dislocations. The dislocation line forms a jog that features a sessile edge component. Creation of a trail of point defect causes a resulting drag force on the dislocation which results in a bowing out of the segment. Because of the specific Burgers vectors of the intersecting dislocations and the line orientation, the cutting dislocations only have a small screw component equal to $\sqrt{6}/12a_0$ (half the length of a partial Burgers vector). Therefore, not a complete point defect is generated but rather a trail of local lattice distortion, a phenomenon we will refer to as a trail of partial point defects. The defect has a dipole structure, and is depicted in Fig. 2(c). The dragging force of the trail of partial point defects was estimated by calculating the energy per length for a trail of partial point defects and that of a vacancy tube, and it is calculated to be about 20% of that of a complete vacancy tube. This defect thus causes a significant dragging force on the dislocations, in particular in a situation where the dislocation density is extremely high as in the present simulation. This could potentially become important in high strain rate situations such as explosive conditions.

Two representative dislocation-cutting processes are schematically shown in Fig. 3. The forces on the jog segment are a combination of tensile and compressive forces in the two $\langle 112 \rangle$ directions. This immediately explains the dipole structure seen in Fig. 2(c). The bowing effect on the dislocations is shown in Figs. 4(a)and 4(b), based on a centrosymmetry analysis in Fig. 4(a), and on an energy analysis in Fig. 4(b). To our knowledge, the trail of partial point defects has not been described previously.

Thus far we have only discussed the reactions that take place when dislocations of the same clouds react. Numerous dislocation reactions occur when dislocations of the two different clouds start to interact, as shown in Fig. 4(c). Such reactions primarily involve dislocation-cutting processes as depicted schematically in Fig. 2(a). Due to the Burgers vectors and the dislocation line orientation, when the dislocation clouds meet straight ahead of the crack, the reactions are

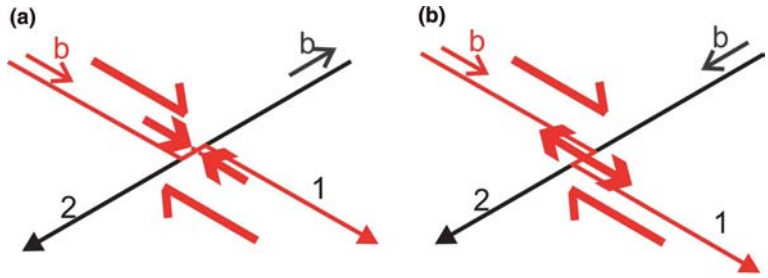

Fig. 3 Generation of point defects due to jogs in screw dislocations. Two representative dislocation-cutting processes are shown, (**a**) leading to formation of an interstitial, (**b**) leading to formation of vacancy tubes. In case the edge component of the jog is smaller than that of a partial Burgers vector, trails of partial point defects, characterized by generation of local lattice distortion rather than complete rows of missing or additional atoms, are generated

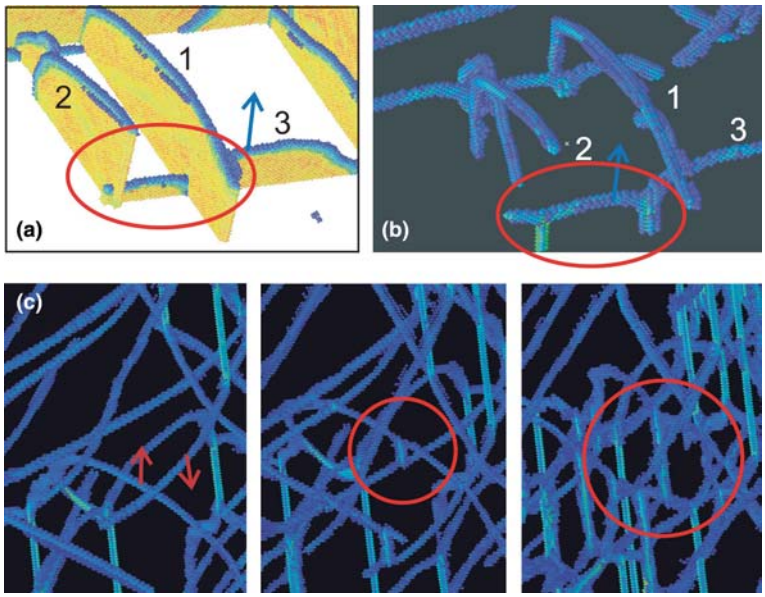

Fig. 4 Generation of trails of point defects in early stages of the simulation. Dislocation number 1 and number 2 leave a stacking fault plane, which is subsequently cut by dislocation number 3. Therefore, two trails of partial point defects are generated resulting in bowing of dislocation number 3 (see the mechanism shown in Fig. 2(b)). Subplot (**a**) shows a centrosymmetry analysis [25] where the stacking fault planes are drawn yellow; subplot (**b**) shows an energy analysis of the same region where the stacking fault planes are not shown. Panel (**c**) shows the reaction of the two dislocation clouds originating from opposing crack tip causing generation of numerous point defects

very similar to those observed in the previous stages when dislocations of the same clouds cut each other's stacking fault and thus, trails of partial point defects are generated. In Fig. 4(c), the significant effect of jog dragging on the motion of the dislocations is clearly observed. The elastic interaction of dislocations repelling each other causes a decrease in the dislocation velocity.

Due to the crystal orientation and the Burgers vector of the dislocations, only trails of partial point defects as well as interstitials can be generated from the cutting processes on the primary glide systems.

Complete vacancy tubes [13, 14, 26] are not generated until later stages of the simulation when the dislocation density becomes very large and secondary slip systems are activated (see discussion in the next section). A large number of such defects are created and appear as straight, thick lines in the plot of the potential energy of atoms. The geometry of complete vacancy tubes is shown in Fig. 2(d). The vacancy tubes observed in the simulation are only several nanometres long. We also observe formation of some trails of interstitials. The number of such processes is rather small since the energy to create such defects is extremely large. A trail of interstitials is depicted in Fig. 2(e). The excess of vacancy concentration is also found in experiments of materials under heavy plastic deformation [17, 27, 28]. More recently, there are also several observations of vacancy generation in computer simulations [13, 17–19, 29]. In particular, the study reported in Ref. [17] shows formation of single vacancy tube due to dislocation cutting processes.

3.3 Activation of Secondary Slip Planes

We observe that secondary slip systems are activated once the dislocation density is above a critical value. Figures 5(a)–5(d) illustrates activation of secondary slip systems.

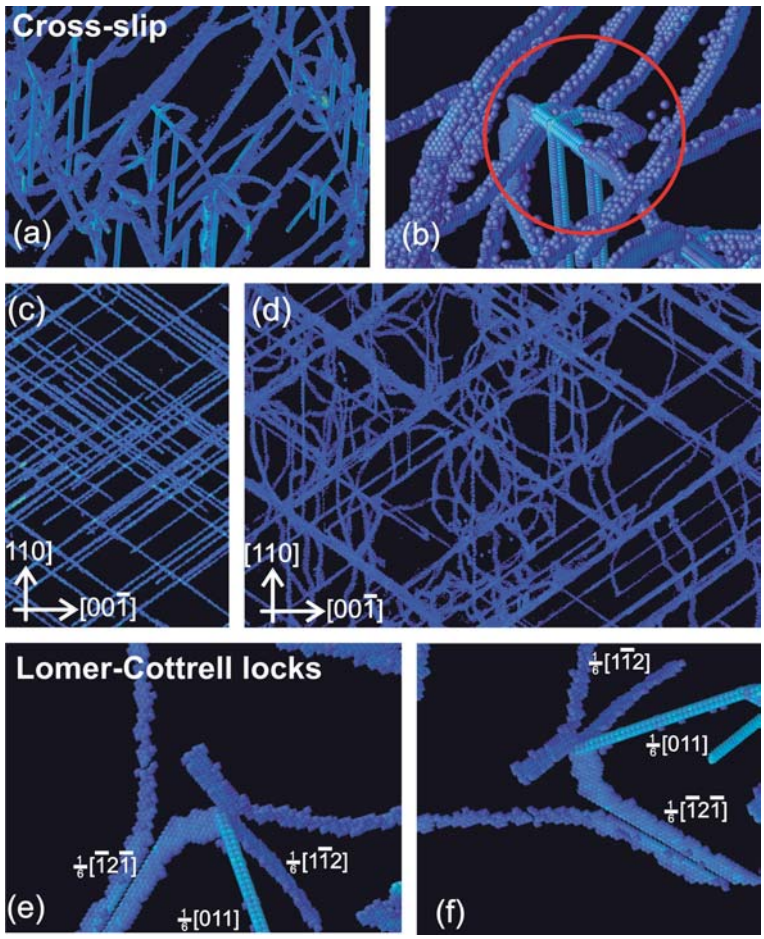

Fig. 5 Activation of secondary slip systems and generation of Lomer-Cottrell locks. Plots (a) and (b) show details of activation of secondary slip systems (subplot (b) is a magnified view of subplot (a)). This mechanism of cross-slip of partial dislocations, here first observed in MD simulation, was originally proposed theoretically by Fleischer [30], and contrasts the well-known Friedel-Escaig mechanism [1]. Subplots (c) and (d) show a view from the [1$\bar{1}$0]-direction (c) before nucleation of dislocations on secondary glide systems (therefore only straight lines), and (d) after nucleation of dislocations on secondary glide systems (which appear as curved lines). Subplots (e) and (f) show detailed views on the formation of sessile Lomer-Cottrell locks, with its typical shape of a straight sessile arm connected to two partial dislocations

In the simulation, we find that dislocations on secondary slip systems are generated by cross slip and Frank-Read mechanisms. This is an unexpected observation because cross slip is only possible, according to the classical dislocation mechanics, along at least locally constricted screw segments (Friedel-Escaig's mechanism) [1]. Due to the low stacking fault energy of the model material used here, only partial dislocations exist in our simulation. Each occurring cross-slip event leaves behind a straight, sessile stair-rod dislocation to conserve the Burgers vector. These sessile segments can clearly be observed in Figs. 5(a)–5(d). The main result is that by this novel mechanism it is possible to observe cross-slip in a situation when only partial dislocations, together with very high stresses are present. Even in systems with only partial dislocations, nature finds a way to relieve elastic energy into secondary slip systems! We note that this mechanism of cross-slip of partial dislocations was proposed in 1959 by Fleischer [30]. Our simulation is – to our knowledge – the first computer simulation that confirms the existence of such mechanism.

Activation of secondary slip systems is important for the hardening process because dislocation cutting or the formation of sessile locks generates a large number of additional defects. Dislocations on secondary slip systems cannot move easily in the beginning. However, soon afterwards, numerous new defects are generated. In particular, we observe formation of complete vacancy tubes at this stage dramatically increasing the concentration of vacancies. We note that cross-slip mechanisms have been studied in other MD simulations previously [31–33]. In contrast to these works, in our study we observe cross slip competing with numerous other dislocation mechanisms.

3.4 Formation of sessile locks

Another mechanism of dislocation interactions is formation of sessile locks. An analysis of the Burgers vectors of the primary dislocations reveals that formation of sessile locks is not observed until dislocations on secondary glide planes are activated.

Sessile dislocation locks can be formed depending on the Burgers vector whenever two partial dislocations on different glide planes get close together. Some combinations of partial dislocations are attractive and form a dislocation line with Burgers vector of the type 1/6[110]. These dislocations are not glissile on any glide system of the FCC lattice, and therefore it is sessile and cannot move. Such defects provide a serious burden for further dislocation glide through the material, since other dislocations approaching the sessile dislocations cannot easily glide through this defect agglomerate, or the so called Lomer-Cottrell lock. One of the possibilities is how such locks may be circumvented by Orowan-mechanisms [1, 3].

Formation of sessile dislocations is also observed in the simulation. It is found that the sessile dislocations severely hinder further dislocation motion, as it is assumed in the classical theories of work hardening [1]. In Figs. 5(e) and 5(f) we show some snapshots when such defects are generated. The typical structure of the Lomer-Cottrell lock is characterized by a straight sessile arm connected with two partials on different glide planes. This can be clearly seen in the figure. Formation of Lomer-Cottrell locks has been studied in previous MD simulation [34], but, as discussed in the previous section, not in competition with other mechanisms. Formation of sessile locks has recently also been found in deformation of nanocrystalline materials [23,24].

3.5 The work-hardening regime

The simulation reveals the final sessile structure of a large number of dislocations in the late stages of the plastic deformation. When a situation is reached where the plastic deformation of a solid has generated such a high dislocation density that dislocation motion is hindered by their mutual interactions, one generally speaks of the work-hardening regime of deformation. In the molecular dynamics simulation the deformation is large enough that this work-hardening regime is reached quickly. In this final stage, we see a structure composed of point defects, sessile dislocations and partial dislocations. This geometric arrangement explains the particular structure dominated by the straight defect segments in the final stages of simulation.

Several views onto this final stage are shown in Fig. 6(a), revealing the final network from a distant view. The blow-up in Fig. 6(a) shows a more detailed energy analysis of the network. The characteristic structure of the network is due to the fact that all sessile defects (trails of point defects as well as 1/6[110]-sessile dislocations as part of the Lomer-Cottrell locks) assume tetrahedral angles and lie on the edges of Thompson's tetrahedron. This immediately explains the particular structure of the observed sessile network.

In contrast to the initial stages of plastic deformation, where dislocation glide occurred easily, dislocation motion is essentially stopped due to the work hardening and plastic relaxation.

4 Discussion

We observe that dislocation-cutting processes generate a large number of trails of point defects. An interesting aspect is observation of generation of trails of partial point defects by dislocation cutting processes with an orientation such that the sessile edge component of the jog is relatively small. This does not cause generation of a complete row of vacancies or interstitials, but rather a local lattice distortion (see Fig. 2(c)). This defect has, to the best of our knowledge, not been described and observed previously. As we have shown by our simulation, it has an important effect on hindering free dislocation motion. Such deformation mode could become important in nanostructured materials, where it is now understood that partial dislocations can dominate plastic deformation [8–11]. Indeed, in some MD simulations of nanocrystalline materials, similar cutting mechanisms as described in the present work have been observed [9–11,22, 24].

Once the dislocation density in the center of the solid grain exceeds a critical value, dislocations on secondary slip systems are activated. Since only partial dislocations are present in the current study, the dislocations must leave a sessile dislocation segment to conserve the Burgers vector (see Fig. 5(b)). Such mechanism of partial dislocation cross slip was actually proposed theoretically almost 50 years ago [30], and rediscovered by our MD simulation.

Another important dislocation reaction mechanism is the formation of sessile Lomer-Cottrell locks (see Figs. 5(e) and 5(f)). Formation of sessile locks is not observed until dislocations on secondary glide planes are activated.

We observe formation of complete vacancy tubes once secondary slip systems are activated (see Fig. 2(d)). The observation of generation of vacancies is in agreement with the understanding that heavy plastic deformation causes generation of vacancies. Mott [26] was the first to predict the vacancy formation by motion of jogged screw dislocations. The production of vacancies [27] and their influence on plasticity has been studied in experiment and theory [13–15,18, 29,35], and has also been included in discrete dislocation modelling recently [15].

Figure 6(b) plots the development of the density of different defects during the simulation using a method of separating defects of different energies. The potential energy of atoms allows discrimination between different types of defects. This figure summarizes the hardening process in our simulation. At the first stage, partial dislocations are emitted from cracks with a high rate. As a consequence of cutting processes trails of point defects are produced. Finally, the activation of secondary glide systems results in additional dislocation cutting processes including the generation of complete vacancy tubes. Another important hardening mechanism is formation of sessile dislocations. It is interesting to note that the rapid production of defects ceases, with the creation of cutting debris (and the plastic relaxation). The density of defects finally goes into an equilibrium. The density of partial dislocations increases rapidly until $t \approx 300$ where a maximum is reached

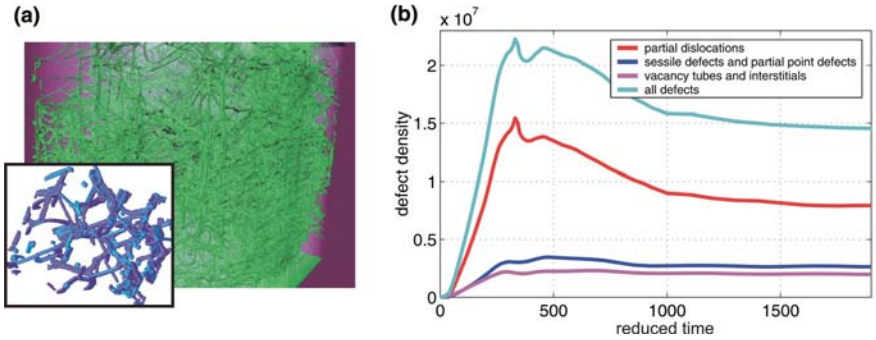

Fig. 6 Subplot (**a**) The final network from a distant view, including a blow-up to show the details of the network. The characteristic structure of the network is due to the fact that all sessile defects (both trails of partial and complete point defects) as well as -sessile dislocations as part of the Lomer-Cottrell locks assume tetrahedral angles and lie on the edges of Thompson's tetrahedron 1, 2. The wiggly lines in the blow-up show partial dislocations, and the straight lines correspond to sessile defects. Subplot (**b**) Development of the density of different defects during the simulation. The defect densities are approximated based on an energy criterion. Atoms associated with partial dislocations have an energy between -6.1 and -5.9, sessile defects as well as trails of partial point defects have potential energy between -5.9 and -5.75 and vacancy tubes and trails of interstitials have an energy higher than -5.6

after which the density decreases and reaches a plateau value in the long-time limit. This corresponds to the point when sessile locks are formed and thus the total line length of partial dislocations is reduced. In agreement with this observation, the density of sessile defects and partial point defects continues to increase up to $t \approx 490$, thus far beyond the time when the maximum of partial dislocation density is reached. The density of interstitials and vacancy tubes increases up to $t \approx 250$ and levels off at a plateau value.

5 Summary and conclusions

The main contributions of this paper are:

(1) We have shown the concurrent dynamics of fundamental mechanisms of work hardening [1–3], in a single computer simulation, including: (1) dislocation cutting processes, (2) cross-slip, and (3) formation of sessile dislocation locks. This is in contrast to many previous studies, where only single mechanisms have been studied (see, for example Refs. [18, 19, 22–24, 33]). The dynamical evolution of defect densities could be correlated with the time evolution of these events as shown in Fig. 6(b).
(2) We have discovered a new class of point defects referred to as trail of partial point defects, which could play an important role in situations when partial dislocations dominate plasticity (see Fig. 2(c)).
(3) We have rediscovered the Fleischer-mechanism of cross-slip of partial dislocations that contrasts the well-known Friedel-Escaig mechanism [30]. The Fleischer mechanism was theoretically proposed more than 50 years ago, but so far not confirmed by computer simulation or experiment.
(4) Our study also exemplifies methods to analyze ultra-large scale simulations. Similar techniques, based on energy filtering, usage of the centrosymmetry parameter, and geometrical analysis may be a fruitful approach for future investigations of ultra-large scale studies of materials failure.

An important result is that the collective operation of the basic hardening mechanisms apparently constricts the mobility of dislocations. A large ensemble of defects self-organizes into a complex defect network with a regular structure leading to a final defect network composed of trails of partial point defects and complete vacancy tubes as well as some trails of interstitials, sessile dislocations, and partial dislocations. The characteristic structure of the final network is given by the geometrical condition that the sessile defects appear as straight lines lying at the intersection of stacking faults, thus along the sides of Thompson's tetrahedron.

The results illustrate that even though the LJ potential is a simplistic model for interatomic bonding, it is nevertheless capable of capturing most of the predicted hardening mechanisms [1–3]. A computer simulation using the LJ potential under extreme conditions of very large strains seems to be able to reproduce the essential deformation mechanisms of natural crystalline materials such as metals.

However, in MD simulations, systems are generally under relatively "harsh" conditions, such as high stress and strain rates. This may lead to activation of all of the possible dislocation mechanisms, whereas under more realistic conditions, the system discriminates between the different mechanisms, then favoring the lowest-energy path. Therefore, although MD simulation can elucidate the possible mechanisms, experimental verification of the rate limiting processes remains a critical issue. In this spirit, our MD experiments could thus be viewed as informative, but not representative of the hardening mechanisms under more normal conditions, and the results should be interpreted with care.

To investigate the hardening mechanisms with more realistic potentials for metals, we have conducted additional simulations of work-hardening using potentials developed within the EAM framework. Notably, we observe similar hardening mechanisms as discussed in this paper. In particular, dislocation cutting processes, cross-slip and formation of sessile locks play a dominating role.

We emphasize that such detailed atomistic views on fundamental aspects of plasticity, as shown in our study, can be

obtained neither from experimental techniques, nor can they be calculated with continuum mechanics methods, especially in view of extremely high dislocation densities and strain rates. In this respect, with its limitations understood, MD simulations are a unique way to obtain such information.

Acknowledgements Farid F. Abraham wishes to acknowledge the generous support provided by the Humboldt Research Award for Senior US Scientists and a computer grant at the San Diego Supercomputer Center. The work of Mark A. Duchaineau was performed under the auspices of the U.S. Department of Energy by University of California Lawrence Livermore National Laboratory under contract No. W-7405-Eng-48. We are grateful to Dr. Vasily V. Bulatov of Lawrence Livermore National Laboratory for providing helpful comments during preparation of the manuscript.

References

1. Hirth, J.P., Lothe, J. : Theory of Dislocations. Wiley-Interscience, 1982
2. Hull, D., Bacon, D.J.: Introduction to Dislocations. Butterworth Heinemann, 2002
3. Courtney, T.H.: Mechanical behavior of materials. McGraw-Hill, 1990
4. Allen, M.P., Tildesley, D.J.: Computer Simulation of Liquids. Oxford University Press, 1989
5. Abraham, F.F., Walkup, R., Gao, H. et al.: Simulating materials failure by using up to one billion atoms and the world's fastest computer: Work-hardening. P. Natl. Acad. Sci. USA, **99**(9): 5783–5787 (2002)
6. Gumbsch, P., Gao, H.: Dislocations faster than the speed of sound. Science, **283**: 965–968 (1999)
7. Buehler, M.J., Abraham, F.F., Gao, H.: Hyperelasticity governs dynamic fracture at a critical length scale. Nature, **426**: 141–146 (2003)
8. Wolf, D., Yamakov, V., Phillpot, S.R. et al.: Deformation mechanism and inverse Hall-Petch behavior in nanocrystalline materials. Z. Metallk., **94**: 1052–1061 (2003)
9. Yamakov, V., Wolf, D., Phillpot, S.R., Mukherjee, A.K. et al.: Dislocation processes in the deformation of nanocrystalline aluminium by MD simulation. Nature Materials, **1**: 1–4 (2002)
10. van Swygenhoven, H., Derlet, P.M., Hasnaoui, A.: Atomic mechanism for dislocation emission from nanosized grain boundaries. Phys. Rev. B, **66**: 024101 (2002)
11. Farkas, D., van Swygenhoven, H., Derlet, P.: Intergranular fracture in nanocrystalline metals. Phys. Rev. B, **66**: 060101 (2002)
12. Derlet, P.M., Hasnaoui, A., van Swygenhoven, H.: Atomistic simulations as guidance to experiments. Scripta Mater., **49**: 629–635 (2003)
13. Schiotz, J., Leffers, T., Singh, B.N.: Dislocation nucleation and vacancy formation during high-speed deformation of fcc metals. Phil. Mag. Lett., **81**: 301–309 (2001)
14. Jacobsen, K.W., Schiotz, J.: Computational materials science - nanoscale plasticity. Nature Materials, **1**: 15–16 (2002)
15. Rhee, M., Zbib, H.M., Hirth, J.P. et al.: Models for long-/short-range interactions and cross slip in 3D dislocation simulation of bcc single crystals. Modeling Simul. Mater. Sci. Eng., **6**(4): 467–492 (1998)
16. Wen, M., Lin, D.L.: Atomistic process of dislocation cross-slip in Ni3Al. Scripta Mater., **36**: 265–268 (1997)
17. Zhou, S.J., Preston, D.L., Louchet, F.: Investigation of vacancy formation by a jogged dissociated dislocation with large-scale molecular dynamics and dislocation energetics. Acta Mater., **47**: 2695–2703 (1999)
18. Li, M., Zhou, S.J.: Investigation of jog motion in gamma-TiAl via molecular dynamics. Phil. Mag. Lett., **79**: 773–784 (1999)
19. Li, M., Chu, W.Y., Qian, C.F. et al.: Molecular dynamics simulation of dislocation intersections in aluminum. Mat. Sci. Eng. A, **363**: 234–241 (2003)
20. Zhou, S.J., Preston, D.L., Lomdahl, P.S. et al.: Large-scale molecular-dynamics simulations of dislocation interactions in copper. Science, **279**: 1525–1527 (1998)
21. Bulatov, V., Abraham, F.F., Kubin, L. et al.: Connecting atomistic and mesoscale simulations of crystal plasticity. Nature, **391**: 669–672 (1998)
22. Schiotz, J., Jacobsen, K.W.: A maximum in the strength of nanocrystalline copper. Science, **301**: 1357–1359 (2003)
23. Yamakov, V., Wolf, D., Phillpot, S.R. et al.: Dislocation-dislocation and dislocation-twin reactions in nanocrystalline Al by molecular dynamics simulation. Acta Mat., **51**: 4135–4147 (2003)
24. Yamakov, V., Wolf, D., Phillpot, S.R. et al.: Deformation-mechanism map for nanocrystalline metals by molecular dynamics simulation. Nature Materials, **3**: 43–47 (2004)
25. Kelchner, C., Plimpton, S.J., Hamilton, J.C.: Dislocation nucleation and defect structure during surface-indentation. Phys. Rev. B, **58**: 11085–11088 (1998)
26. Mott, N.F.: The work hardening of metals. Trans. Met. Soc. AIME, **218**: 962 (1960)
27. Krause-Rehberg, R., Brohl, M., Leipner, H. et al.: Defects in plastically deformed semiconductors studied by positron annihilation: Silicon and germanium. Phys. Rev. B, **47**: 13266–13276 (1993)
28. Rempel, A.A., Nazarova, S.Z., Gusev, A.I.: Intrinsic defects in palladium after severe plastic deformation. Phys. Stat. Sol., **181**: R16 (2000)
29. Marian, J., Cai, W., Bulatov, V.V.: Dynamic transitions from smooth to rough to twinning in dislocation motion. Nature Materials, **3**: 158–163 (2004)
30. Fleischer, R.L.: Cross slip of extended dislocations. Acta Metall., **7**: 134–135 (1959)
31. Qi, Y., Strachan, A., Cagin, T., Goddard, W.A.: Large-scale atomistic simulations of screw dislocation structure, annihilation and cross-slip in FCC Ni. Mat. Sci. Eng.A, 309–310, 156–159 (2001)
32. Vegge, T., Jacobsen, W.: Atomistic simulations of jog migration on extended screw dislocations. Mat. Sci. Eng. A, 319–321 , 119–123 (2001)
33. Vegge, T., Jacobsen, W.: Atomistic simulations of dislocation processes in copper. J. Phys. Condens. Matt., **14**: 2929–2956 (2002)
34. Shenoy, V.B., Kukta, R.V., Phillips, R.: Quasicontinuum models of interfacial structure and deformation. Phys. Rev. Lett., **84**: 1491–1494 (2000)
35. Hirsch, P.B., Warrington, D.H.: The flow stress of aluminium and copper at high temperatures. Phil. Mag., **6**: 735 (1961)